PHYSICAL REVIEW B VOLUME 61, NUMBER 6 1 FEBRUARY 2000-II

Electrical transport and magnetic properties of a possible electron-doped layered manganese oxide

Y. G. Zhao,* Y. H. Li, S. B. Ogale, M. Rajeswari, V. Smolyaninova, T. Wu, A. Biswas, L. Salamanca-Riba, R. L. Greene, R. Ramesh, and T. Venkatesan

Center for Superconductivity Research, Department of Physics, University of Maryland, College Park, Maryland 20742

J. H. Scott

National Institute of Standards and Technology, Gaithersburg, Maryland 20899

(Received 9 June 1999; revised manuscript received 26 August 1999)

We report on the structural, transport, and magnetic properties of $La_{0.67}Sr_{0.33}MnO_x$ thin films grown in vacuum by pulsed-laser deposition. The as-grown thin films have both the matrix $La_{1.34}Sr_{0.66}MnO_4$ phase with K_2NiF_4 structure and an embedded MnO phase. The electrical transport and magnetic properties of the films are determined mainly by those of the matrix phase. By annealing, the as-grown thin films can be transformed into the normal $La_{0.67}Sr_{0.33}MnO_3$ single phase, which shows the expected colossal magnetoresistance effect. Based on the composition of the matrix phase, and the structural, electrical, and magnetic properties of the films, we propose that the matrix phase is possibly electron doped with a mixed valence of Mn^{2+}/Mn^{3+} instead of the Mn^{3+}/Mn^{4+} as in the hole-doped case.

INTRODUCTION

Rare-earth manganese oxides of the form $L_{1-x}A_xMnO_3$ (L = rare-earth elements, A = alkaline-earth elements) have attracted much interest due to their importance for both basic research and applications.[1–3] These materials show various unusual properties, such as colossal magnetoresistance (CMR), charge and orbital ordering, etc.[4] It has been shown that the spin, charge, and lattice are strongly coupled in these compounds.[5–8] Much work has been done regarding the L site doping, while relatively little work has been done on the effect of oxygen content on the structural, transport, and magnetic properties. Because of the strong interaction among spin, charge and lattice in CMR materials, it can be expected that the effect of changing oxygen content may be quite different from that of L site doping, although they may give the same number of carriers.

Ju *et al.*[9] studied the effect of oxygen content on the transport and magnetic properties of La-Ba-Mn-O bulk materials by using a Ti getter to change the oxygen content in the samples, and the change in the transport and magnetic properties was found to be dramatic. It is not easy to change the oxygen content of bulk materials and the homogeneity is always an issue. Goyal *et al.*[10] studied $La_{0.7}Ca_{0.3}MnO_3$ thin films deposited under different oxygen pressures (10–50 Pa, or 75–400 mTorr), but all cooled under the same oxygen pressure (50 000 Pa, or 400 Torr). The electrical transport and magnetic properties showed some changes which could be due to the differences in the oxygen content in the samples, but these changes were not dramatic. A number of questions arise naturally. If we prepare the thin films in vacuum, can we obtain the same structural phase? What are the electrical transport and magnetic properties of the phase? Can we drive the samples to the electron-doped character by strongly reducing the oxygen content to produce Mn^{2+}/Mn^{3+}, instead of Mn^{3+}/Mn^{4+}?

EXPERIMENT

Thin films of nominal composition $La_{0.67}Sr_{0.33}MnO_x$ were grown in vacuum on (001) $LaAlO_3$ substrates by pulsed-laser deposition (laser wavelength of 248 nm) using a high-quality $La_{0.67}Sr_{0.33}MnO_x$ target. The laser energy fluence and the substrate temperature used were 2 J/cm^2 and 800 °C, respectively. The pulse repetition frequency of deposition was 8 Hz. The films were deposited and cooled down in vacuum (6.40×10^{-3} Pa, or 4.8×10^{-5} Torr). The deposition rate is approximately 0.22 nm/s. The thickness of the films was about 150 nm as measured by Rutherford back scattering. X-ray diffraction (XRD) was used for phase and crystallinity analysis. The measurements were made using a monochromated Cu $K\alpha$ source (not a beta filter), a 175 mm radius goniometer in the θ–2θ geometry, and constant slit width. Transmission electron microscopy (TEM) and energy-dispersive x-ray spectrometry (EDS) were used to study the composition of the film and the microstructure. A linear four-point probe was used to measure the transport properties of the thin films from room to liquid-helium temperature. Resistivity of the annealed thin films was measured with in-plane magnetic fields of 4 and 8 T in order to show the CMR effect. Because of the high resistance of the vacuum-prepared samples, an electrometer was also used for the transport measurement. A superconducting quantum interference device magnetometer was used to measure the temperature and field dependence of magnetization with samples mounted in a plastic soda straw. The magnetic field was parallel to the film surface. Both zero-field cooling (ZFC) and field-cooling (FC) data were recorded.

RESULTS AND DISCUSSION

Figure 1(a) shows the x-ray diffraction pattern of the $La_{0.67}Sr_{0.33}MnO_x$ thin films prepared in vacuum, which shows five peaks within the range of 10–80° for 2θ, in addition to three substrate peaks. The pattern in Fig. 1(a) is

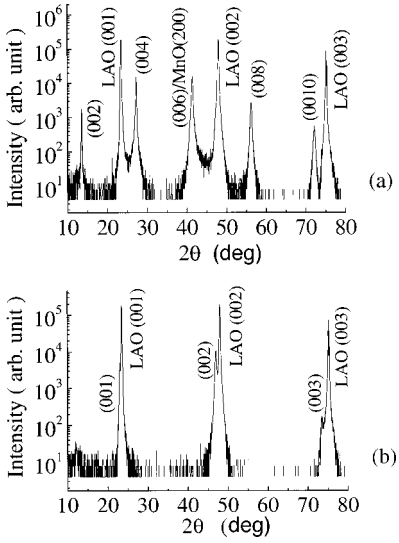

FIG. 1. X-ray-diffraction patterns of vacuum-prepared $La_{0.67}Sr_{0.33}MnO_x$ thin films (a) before and (b) after annealing in flowing oxygen at 800 °C for 10 h.

quite different from that of the normal $La_{0.67}Sr_{0.33}MnO_x$ thin films which are prepared in oxygen. The ratio of the *d* spacings calculated for the five sample peaks using Bragg law is 1:2:3:4:5, so they belong to the same reflection group. This, along with the absence of other peaks in the diffractogram, suggests that the films are single phase. Figure 1(b) shows the x-ray-diffraction pattern for the same vacuum-prepared $La_{0.67}Sr_{0.33}MnO_x$ thin films, subsequently annealed at 850 °C for 10 h in flowing oxygen. It shows an XRD pattern similar to that of the normal $La_{0.67}Sr_{0.33}MnO_x$ thin films prepared in oxygen, which show the CMR effect. These results establish that the vacuum-prepared $La_{0.67}Sr_{0.33}MnO_x$ thin films have distinctly different XRD patterns from the normal $La_{0.67}Sr_{0.33}MnO_x$ thin films, but can be transformed into the normal phase by oxygen annealing.

Figure 2(a) shows the TEM plan view image of the vacuum-prepared $La_{0.67}Sr_{0.33}MnO_x$ thin film in the as-grown state along with a [001] zone-axis electron-diffraction pattern from the same material. It can be seen from the image that a square-shaped second phase is distributed throughout the film, and the boundaries between the second phase and the matrix phase are highly strained. EDS measurements indicate that the second phase contains only Mn and oxygen, which implies that it is a form of manganese oxide. The diffraction pattern in the inset of Fig. 2(a) shows two sets of diffraction spots. One set can be indexed as MnO, which displays complete overlap with the peaks from the matrix phase along the *c* axis in the XRD pattern of the films (one overlap every three peaks), which is why the XRD pattern of the films seems to show a single phase. This is also confirmed in the electron diffraction along [100], which only shows two sets of diffraction spots along one direction. This TEM result shows that there are two distinct structures in the vacuum-prepared $La_{0.67}Sr_{0.33}MnO_x$ thin films, and the two structures have different lattice parameters a, b, but have commensurate relation in lattice parameter c. Figure 2(b) shows a high-resolution image of the thin films in cross section, revealing a columnar second phase embedded in the matrix phase with the width of the columns ~20 nm. By

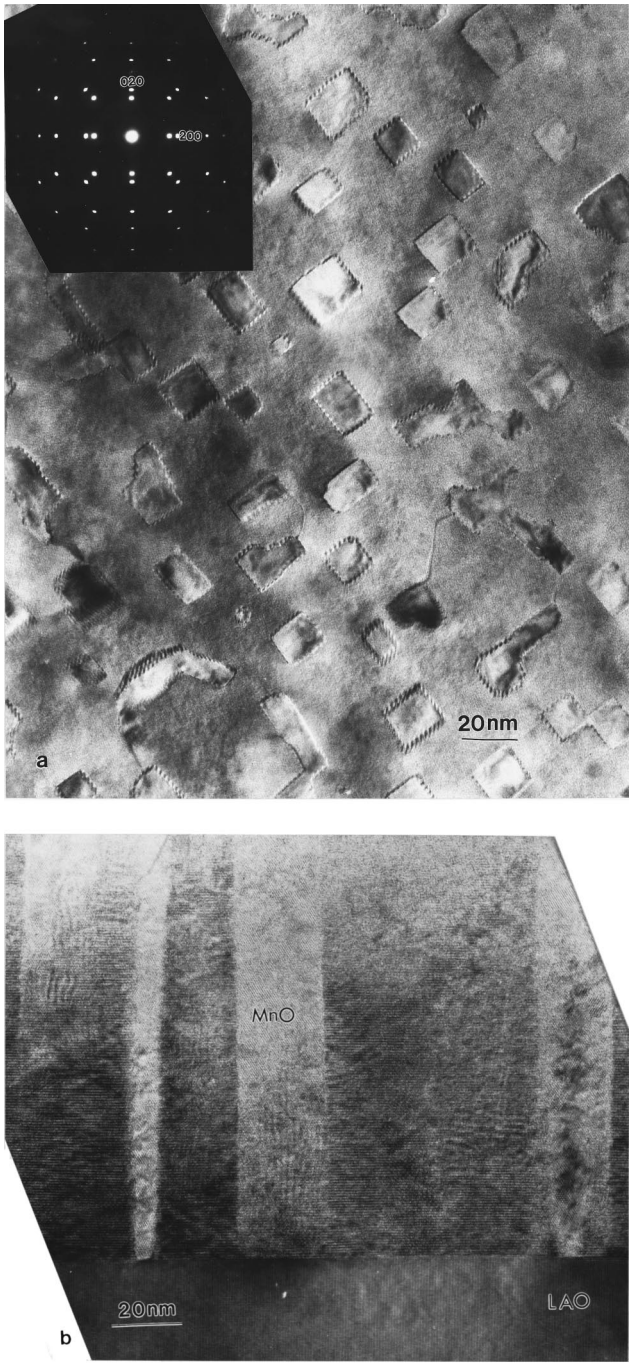

FIG. 2. (a) Plan view image of the vacuum-prepared $La_{0.67}Sr_{0.33}MnO_x$ thin films. Inset shows the electron diffraction along [001]; the index of the diffraction spots is for MnO. (b) High-resolution image of a cross section of the vacuum-prepared $La_{0.67}Sr_{0.33}MnO_x$ thin films.

comparing the TEM and XRD results with the known manganese oxides, it can be deduced[11] that the columnar phase is MnO, while the matrix phase is $(La_{0.67}Sr_{0.33})_2MnO_4$, i.e., the $n=1$ layered $(La, Sr)_{n+1}Mn_nO_{3n+1}$ phase,[12] which has tetragonal structure with $a=b=0.3817$ nm and $c=1.322$ nm. The structure of the matrix phase is also confirmed by TEM image simulation which will be published in another paper.[11]

Detailed high-resolution image simulation[11] also indicates that the La and La/Sr layers in our matrix phase are ordered as shown in Fig. 3, which is a significant difference between

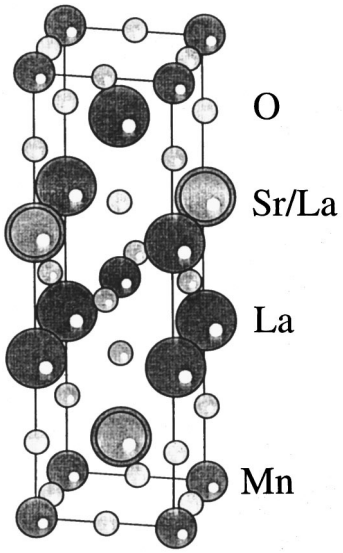

FIG. 3. Structure of the $(La_{0.67}Sr_{0.33})_2MnO_4$ matrix phase.

our matrix phase and the other reported $(La, Sr)_{n+1}Mn_nO_{3n+1}$ phases. Based on the assignments of the two phases, we can index the XRD peaks as shown in Fig. 1. Therefore, we can express the decomposition as $2La_{0.67}Sr_{0.33}MnO_x \Rightarrow (La_{0.67}Sr_{0.33})_2MnO_4 + MnO$. This is proved by the following calculations. MnO has a cubic (f.c.) structure with lattice parameters $a=b=c=0.4445$ nm and $Z=4$ (where Z is the number of molecular units per unit cell),[13] while $(La_{0.67}Sr_{0.33})_2MnO_4$ has a tetragonal structure with $a=b=0.3817$ nm, $c=1.322$ nm and $Z=2$. Therefore, the volume ratio between $(La_{0.67}Sr_{0.33})_2MnO_4$ and MnO should be 4.41:1 if the decomposition formula is correct. The calculated volume ratio between $(La_{0.67}Sr_{0.33})_2MnO_4$ and MnO from the film shown in Fig. 2 is 4.48:1, reasonably consistent with the expected value.

There are some reports about the $n=1$ phase, with composition $La_{1-x}Sr_{1+x}MnO_4$, which claim mixed Mn^{3+}/Mn^{4+} and hole-type carriers.[12,14] The matrix phase in our experiment, with composition $La_{1.34}Sr_{0.66}MnO_4$, belongs to the $La_{1+x}Sr_{1-x}MnO_4$ class with average valence 2.66 for Mn ions. This is consistent with a mixed valence of Mn^{2+}/Mn^{3+} for $La_{1.34}Sr_{0.66}MnO_4$, and suggests the matrix phase is electron doped. While searching for other electron-doped phases, we prepared $La_{0.67}Ca_{0.33}MnO_3$ and $La_{0.8}Sr_{0.2}MnO_3$ thin films in vacuum, but these showed only the normal CMR phase with XRD peaks shifting to lower angles, indicating an increase of the lattice parameters. Therefore, $La_{0.67}Sr_{0.33}MnO_3$ is very unique in this regard. To our knowledge, all previous reports of layered manganese oxides, such as $La_{1-x}Sr_{1+x}MnO_4$ $(n=1)$, $La_{2-2x}Sr_{1+2x}Mn_2O_7$ $(n=2)$, $La_{3-3x}Sr_{1+3x}Mn_3O_{10}$ $(n=3)$, etc.[12] describe hole-doped materials. It has been shown that for hole-doped $La_{1-x}Sr_{1+x}MnO_4$, the c axis d spacing significantly decreases with x from 1.317 nm $(x=0)$ to 1.240 nm $(x=0.6-0.7)$, while the a axis d spacing is nearly independent of x (0.380–0.386 nm).[14] This is in contrast to our matrix $La_{1.34}Sr_{0.66}MnO_4$ phase which has a c lattice parameter (1.322 nm), which is even larger than that of $LaSrMnO_4$ $(x=0)$. This trend in the lattice parameter c lends further support to the idea that the matrix $La_{1.34}Sr_{0.66}MnO_4$ is electron doped. In fact, the preparation condition (vacuum) of the films also favors this idea. Some groups have reported synthesizing $La_2MnO_{4+\delta}$ under reducing conditions.[15,16] For example, Vogel and Johnson *et al.* obtained La_2MnO_4 and MnO by reducing the oxygen content of $La_{0.8}K_{0.2}MnO_3$.[15] It is not clear whether the $La_{1+x}Sr_{1-x}MnO_4$ compounds can only coexist with other compounds, such as MnO, or can exist by themselves.

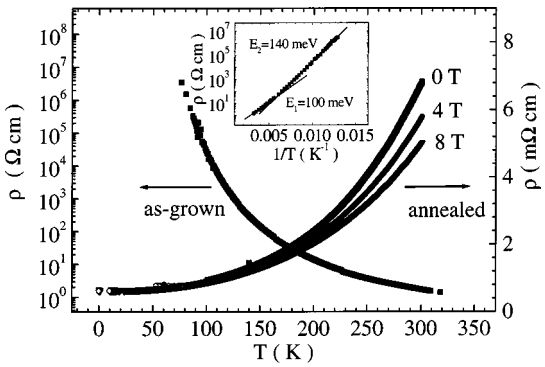

FIG. 4. Temperature dependence of the resistivity for vacuum-prepared $La_{0.67}Sr_{0.33}MnO_x$ thin films before and after annealing. For the annealed thin films, resistivity was measured under 0, 4, and 8 T, respectively. Inset shows $1/T$ dependence of resistivity for vacuum-prepared $La_{0.67}Sr_{0.33}MnO_x$ thin films.

Figure 4 shows the electrical transport properties of the vacuum-prepared $La_{0.67}Sr_{0.33}MnO_3$ thin films before and after annealing. For the as-grown thin films, although they contain both $(La_{0.67}Sr_{0.33})_2MnO_4$ phase and MnO phase, the former dominates the transport property because MnO is an insulator[17] and is embedded in the matrix $(La_{0.67}Sr_{0.33})_2MnO_4$ phase as unconnected inclusions, as seen in Fig. 2(a). Therefore, the transport properties reflect the nature of the $(La_{0.67}Sr_{0.33})_2MnO_4$ phase. The temperature dependence of the film resistivity is comparable to that in the hole-doped $La_{0.7}Sr_{1.3}MnO_4$ single crystals.[14] The inset of Fig. 4 shows $1/T$ dependence of the resistivity for the thin films before annealing. It shows two thermally activated transport processes with activation energies of 100 and 140 meV, respectively. The intersection temperature, where the linear fits cross, is about 175 K, which is very close to the temperature where magnetization begins to increase, as shown by the magnetic measurements given below. The implication is that the transport activation energy of the carriers is affected by the magnetization change and the mechanism of this correlation needs further study. It should be mentioned that we did not substract the volume of MnO when calculating the resistivity. This will increase the resistivity value by about 23% based on the volume ratio between $(La_{0.67}Sr_{0.33})_2MnO_4$ and MnO, but it should not affect the thermal activation energies.

Moritomo *et al.*[14] studied the electrical transport of the hole-doped $La_{1-x}Sr_{1+x}MnO_4$ materials. Their results show that the parent compound $LaSrMnO_4$ $(x=0)$ exhibits insulating behavior with a thermal activation energy of 70 meV. Sr doping reduces the resistivity, but when x exceeds 0.5, the resistivity begins to increase due to the charge-ordering effect. For our matrix $La_{1.34}Sr_{0.66}MnO_4$ phase, both resistivity and the thermal activation energy (100–140 meV) for electrical transport are much larger than that of $LaSrMnO_4$. Con-

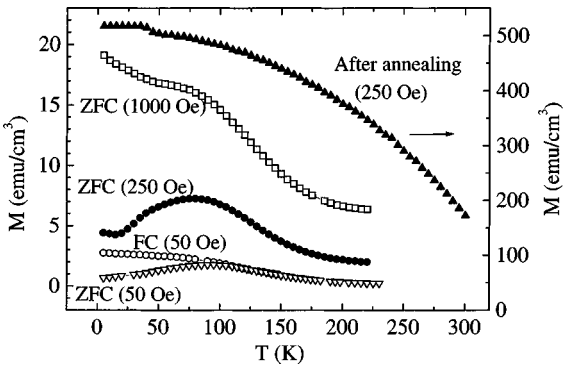

FIG. 5. Temperature dependence of the magnetization for the vacuum-prepared $La_{0.67}Sr_{0.33}MnO_x$ thin films before and after annealing. The substrate contribution has been subtracted.

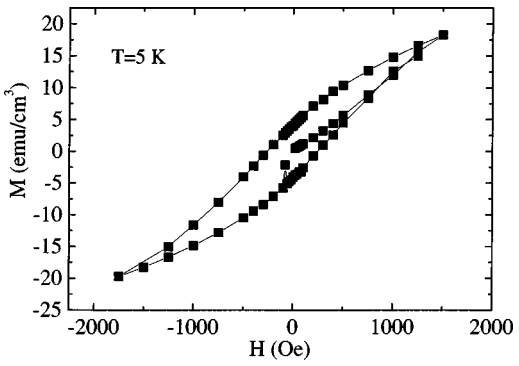

FIG. 6. Magnetic-field dependence of magnetization for vacuum-prepared $La_{0.67}Sr_{0.33}MnO_x$ thin films at 5 K. The substrate contribution has been subtracted.

sidering the composition of the matrix phase this is difficult to explain by assuming that our matrix phase is hole doped.

For the annealed thin films in Fig. 4, the temperature dependence of the resistivity is similar to that of the $La_{0.67}Sr_{0.33}MnO_3$ CMR thin films. The annealed films also show the CMR effect. This is consistent with the XRD results which show that the XRD pattern of the annealed thin films is similar to that of the $La_{0.67}Sr_{0.33}MnO_3$ CMR thin films.

Figure 5 shows the temperature dependence of the magnetization for the vacuum-prepared $La_{0.67}Sr_{0.33}MnO_3$ thin films before and after annealing. For the as-grown films, we measured ZFC magnetization with 3980, 19 900, and 79 600 A/m magnetic fields (50, 250, and 1000 Oe magnetic field, respectively). ZFC and FC curves measured in the magnetic field of 3980 A/m (50 Oe) exhibit difference (hysteresis) as shown in Fig. 5. The ZFC magnetization shows a broad peak around 80 K, whose magnitude decreases with increasing magnetic field. This behavior is consistent with the cluster glass model, which can be described as ferromagnetic clusters embedded in a spin-glass matrix. Inhomogeneity in the as-grown films could produce competing magnetic interactions as well as ferromagnetic clusters, making films magnetically disordered. Magnetization of the as-grown films has contributions from two phases: $(La_{0.67}Sr_{0.33})_2MnO_4$ and MnO. We attribute cluster glass behavior to $(La_{0.67}Sr_{0.33})_2MnO_4$ phase. Pure MnO orders antiferromagnetically at $T_N = 112$ K.[18] Since there is only about 20% of MnO phase in the films, it is difficult to determine whether the MnO phase orders antiferromagnetically (AFM) and at what temperature. The AFM behavior of MnO phase could be masked by the larger magnetic contributions from the $(La_{0.67}Sr_{0.33})_2MnO_4$ phase. In the hole-doped $La_{1-x}Sr_{1+x}MnO_4$ compounds,[14] $LaSrMnO_4$ ($x=0$) shows AF ordering around 120 K (T_N) and T_N decreases with hole doping (x) and vanishes for $x \geqslant 0.2$. For $0.2 \leqslant x \leqslant 0.6$, the samples have a spin-glass phase and the spin-glass transition temperature is not sensitive to the hole doping (x). The AF ordering of the hole doped $La_{1-x}Sr_{1+x}MnO_4$ compounds is not sensitive to the magnetic field, at least up to 1 T, which is in contrast to the behavior of the spin-glass phase ($0.2 \leqslant x \leqslant 0.6$) which is very sensitive to magnetic field and is suppressed below 1 T. For our as-grown thin films, the peak in the $M \sim T$ curves also changes with the magnetic field and this behavior is similar to that of the spin-glass phase in the hole-doped $La_{1-x}Sr_{1+x}MnO_4$. But it is noteworthy that the peak temperature (80 K) in the $M \sim T$ curves for our as grown films is remarkably higher than the spin-glass transition temperature (20 K) for the hole-doped $La_{1-x}Sr_{1+x}MnO_4$. This may be due to the asymmetry of the phase diagrams for the hole-doped and electron-doped compounds. It should also be pointed out that the peak in the magnetization curves is observed at slightly below the Néel temperature of MnO, it may be influenced by the antiferromagnetic phase transition. It is well known that impurities and finite-size effects can reduce magnetic phase transition temperatures, so it is possible that there is some contribution from the AF ordering of MnO. Further work is needed to clarify this issue. For the annealed thin films, the temperature dependence of magnetization and the magnetization value is comparable to that of the normal $La_{0.67}Sr_{0.33}MnO_3$ CMR thin films with T_c above room temperature.

Figure 6 shows the field dependence of the magnetization at 5 K for vacuum-prepared $La_{0.67}Sr_{0.33}MnO_3$ thin films. It shows hysteresis with a coercive field of 19 900 A/m (250 Oe). This is also consistent with a cluster glass behavior. No obvious magnetoresistance (MR) was seen for our as-grown films. This absence of magnetoresistance is consistent with the hole-doped $n=1$ layered manganese oxide $La_{1-x}Sr_{1+x}MnO_4$, which does not show obvious MR either.

In summary, we have grown $La_{0.67}Sr_{0.33}MnO_3$ thin films in vacuum. The films contain both the $La_{1.34}Sr_{0.66}MnO_4$ matrix phase with K_2NiF_4 structure, and a columnar MnO phase. Arguments based on composition, lattice parameter, electrical transport, and magnetic properties suggest that the $La_{1.34}Sr_{0.66}MnO_4$ matrix phase is electron doped. This work may shed light on the synthesis of the possible electron doped, layered CMR materials $(La, Sr)_{n+1}Mn_nO_{3n+1}$, e.g., $La_{2+2x}Sr_{1-2x}Mn_2O_7$ instead of hole-doped $La_{2-2x}Sr_{1+2x}Mn_2O_7$.

ACKNOWLEDGMENTS

We would like to thank J. Gopalakrishnan, R. C. Srivastava, and Chuck Sehmen for discussion and help in this experiment. This work was supported by the NSF MRSEC under Grant No. DMR-9632521.

*On leave from Dept. of Physics, Tsinghua University, Beijing 100084, China. Electronic address: yzhao@squid.umd.edu
[1] S. Chahara, T. Ohno, K. Kasai, and Y. Kozono, Appl. Phys. Lett. **63**, 1990 (1993).
[2] R. von Helmolt, J. Wecker, B. Holzapfel, L. Schultz, and K. Samwer, Phys. Rev. Lett. **71**, 2331 (1993).
[3] S. Jin, T. H. Tiefel, M. McCormack, R. A. Fastnacht, R. Ramesh, and L. H. Chen, Science **264**, 413 (1994).
[4] P. Schiffer, A. P. Ramirez, W. Bao, and S. W. Cheong, Phys. Rev. Lett. **75**, 3336 (1995).
[5] C. Zener, Phys. Rev. **82**, 403 (1951); P. W. Anderson and H. Hasegawa, *ibid.* **100**, 675 (1955); P. G. de Gennes, *ibid.* **118**, 141 (1960).
[6] A. J. Millis, P. B. Littlewood, and B. I. Shraiman, Phys. Rev. Lett. **74**, 5144 (1995); **77**, 175 (1996).
[7] T. T. M. Palstra, A. P. Ramirez, S. W. Cheong, B. R. Zegarski, P. Schiffer, and J. Zaanen, Phys. Rev. B **56**, 5104 (1997).
[8] G. M. Zhao, K. Conder, H. Keller, and K. A. Muller, Nature (London) **381**, 676 (1996).
[9] H. L. Ju, J. Gopalakrishnan, J. L. Peng, Qi Li, G. C. Xiong, T. Venkatesan, and R. L. Greene, Phys. Rev. B **51**, 6143 (1995).
[10] A. Goyal, M. Rajeswari, R. Shreekala, S. E. Lofland, S. M. Bhagat, T. Boettcher, C. Kwon, R. Ramesh, and T. Venkatesan, Appl. Phys. Lett. **71**, 2535 (1997).
[11] Y. H. Li *et al.* (unpublished).
[12] Y. Moritomo, A. Asamitsu, H. Kuwahara, and Y. Tokura, Nature (London) **380**, 141 (1996).
[13] Swanson, *et al.*, NBS Monogr. **539**, 45 (1955).
[14] Y. Moritomo, Y. Tomioka, A. Asamitsu, Y. Tokura, and Y. Matsui, Phys. Rev. B **51**, 3297 (1995).
[15] E. M. Vogel and D. W. Johnson, Thermochim. Acta **12**, 49 (1975).
[16] M. Borlera and Abbattista, J. Less-Common Met. **92**, 55 (1983).
[17] C. Crevecoeur and H. J. De Wit, J. Phys. Chem. Solids **31**, 783 (1970).
[18] T. F. Connolly and E. D. Copenhaver, *Bibliography of Magnetic Materials and Tabulation of Magnetic Transition Temperatures* (Oak Ridge National Laboratory, Oak Ridge, TN, 1969).